A Novel Approach for Connector Modeling and Simulation Using Machine Learning

Hongpeng Zhu, Zaiyong Deng*, Dongwen Chen*, Zhiwei Tan**

***TCL China Star Optoelectronics Technology Co., Ltd. Shenzhen, China**

Abstract

Connectors are key components in signal transmission for high-speed display systems, and their performance is crucial to signal integrity and display quality. However, traditional methods based on 3D FEM(Finite Element Method) simulations and physical testing have limitations in accuracy and efficiency, making it hard to meet the design needs of modern high-speed connectors. To address this, this paper proposes a machine learning model that combines XGBoost regression with Bayesian optimization to predict key performance metrics of connectors, such as insertion loss, return loss, TDR impedance, and eye diagram characteristics. Experimental results show that the method can make accurate predictions in complex conditions and supports a connector transmission bandwidth of 25Gbps, providing an effective solution for high-speed signal channel design.

Author Keywords

Connector(CNT); Insertion loss(IL); Return loss(RL); Eye diagram; XGBoost; Bayesian optimization; Signal Integrity(SI); FEM3D; TV; MNT; NB.

1. Introduction

As TV, MNT and NB display panels become more prevalent in the high-resolution and high-framerate-rate market, designing high-speed signal interfaces (such as DP, HDMI, P2P, and MiniLVDS) is becoming increasingly complex. Data transmission rates are directly proportional to display resolution and frame rate. As data rates continue to rise, connectors, as key nodes in the channel, directly affect the quality of high-speed signal transmission at 25Gbps and above. High-speed signal channels in large-size and high-density display panel products face the following major challenges:

1. The insertion loss and return loss increase significantly, leading to signal attenuation and quality degradation.
2. Impedance discontinuities in the connector region cause signal reflections and distortion.
3. Electromagnetic interference (EMI) and crosstalk issues in high-frequency transmission worsen signal integrity.
4. The decline in eye diagram performance in the signal channel directly increases the bit error rate(BER), affecting display performance.

Currently, the signal integrity design of connectors primarily relies on 3D finite element (FEM) simulations and physical testing, as shown in Figure 1(a). Although these methods offer high accuracy, with the increasingly stringent requirements for signal eye diagram bit error rates(BER), the traditional drawbacks of high computational costs and long time consumption will become bottlenecks in the future connector design, as shown in Figure 2 (b).

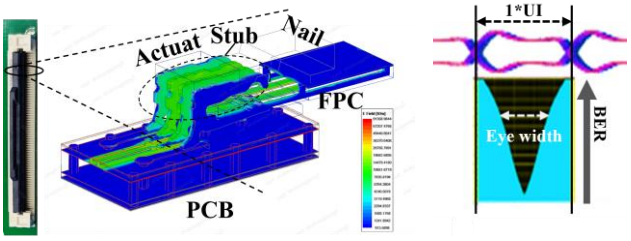

(a) (b)

Figure 1. (a) Connector 3D FEM Electromagnetic Field Simulation; **(b)** Eye Diagram BER Challenges.

To address the challenges mentioned above, this paper proposes an efficient prediction model based on XGBoost regression and Bayesian optimization. Compared to traditional methods, this approach significantly reduces computational costs and time consumption, while effectively adapting to complex multivariable conditions, successfully improving the signal eye diagram. The results show that the model significantly reduces reliance on traditional simulations and testing, improving both prediction efficiency and accuracy, and demonstrating excellent generalization ability.

2. CNT Modeling Factor Analysis

The model is trained using S-parameters extracted from 3D FEM electromagnetic simulations and time-domain transient simulation data. The input features cover the structural and electrical characteristics of the connector, including pin stub length, pin pitch, pin width, dielectric constant, loss tangent, conductivity, surface roughness, PCB and FPC design, and operating frequency, as shown in Table 1. These features comprehensively describe the physical properties and operating environment of the connector, providing a solid data foundation for high-accuracy predictions by the model.[1]

Table 1. CNT/PCB/FFC system characteristics

Item	Parameter	Description	Range	
			min	Max
CNT	Pin_stub	Stub of pin	0mil	110mil
	Pin_pitch	Pitch of pin	0.4mm	1.5mm
	Pin_width	Width of pin	2 mil	14 mil
	Pin_δ	Conductivity of pin	5.8E6	5.8E7
	SR	Surface roughness	0um	10um
	ε	Dielectric constant of actuat/nail	2	5
	tan δ	Loss tangent of actuat/nail	0.002	0.035
PCB & FFC	PCB_Anti pad	Antipad expanding of PCB pad	-2mil	6mil
	EF	Etch factor	0	1

ISSN 0097-996X/25/5601-0464-$1.00 © 2025

Sensitivity analysis is performed based on the feature extraction data using the permutation importance method. This method involves randomly shuffling the values of each input feature and observing the degree of performance degradation to measure the importance of the feature. The greater the performance degradation, the larger the impact of that feature on the target variable.

The analysis results, shown in Figure 2, indicate that pin width and pin pitch have the greatest impact on signal integrity, followed by stub length, dielectric constant and surface roughness. These sensitive features are the focus of subsequent optimization efforts.

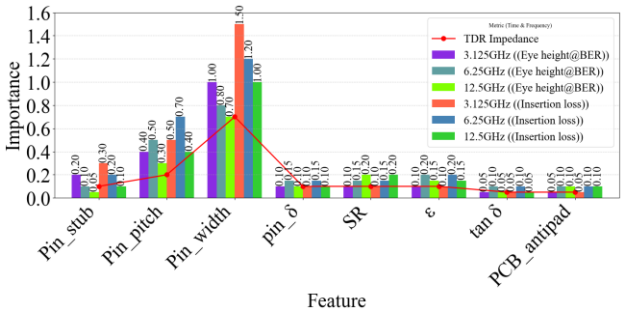

Figure 2. Stacked sensitivity analysis with eye height, insertion loss, and TDR impedance

3. CNT Model Initialization and Validation

The initial connector model was calibrated using the method of extracting equivalent material parameters, which significantly improved the model's accuracy across the entire frequency range. Additionally, the RLGC model was used to validate the feasibility in the low-frequency range, while the S-parameter model was used to describe the distribution parameters in the high-frequency range, accurately capturing the impact of signal reflection caused by the stub.

3.1. CNT Material Parameter Calibration

There are three main reasons for the gap: the difference between the simulation model and the actual model, test errors, and inaccurate material parameters. Connector slicing can correct the simulation model, and test errors can also be eliminated by ISD de-embedding. After that, simulation testing methods are used to fit the equivalent dielectric constant and loss tangent, completing the initialization calibration of the simulation model, as shown in Figure 3.

The reference dielectric distribution in different areas of the connector's metal pins varies, and the dielectric material properties are non-uniformly distributed in space. At the same time, the effects of air dielectric filling and pin surface roughness also need to be considered. The CNT material parameter calibration is completed in the following three steps. [2] [3]

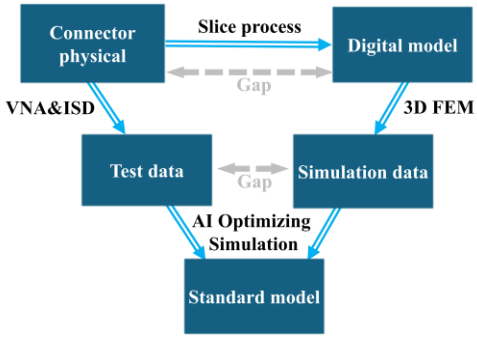

Figure 3. CNT material parameter fitting flowchart.

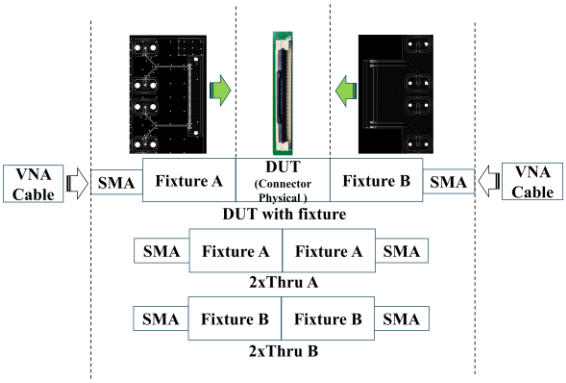

Figure 4. CNT S-parameters testing and ISD de-embedding method.

Step 1: The VNA testing method and S-parameter de-embedding process for the connector are shown in Figure 4. Fixture A and Fixture B were designed and tested, including the de-embedding traces 2xthru A and 2xthru B. Then, the asymmetric de-embedding process was performed using the inverse matrices A^{-1} and B^{-1}, yielding the S-parameter results of the connector with the fixtures removed.

$$DUT\ with\ \ fixture = A \cdot DUT \cdot B \tag{1}$$

$$DUT = A^{-1}A \cdot DUT \cdot BB^{-1} \tag{2}$$

Step 2: Complete the connector pin slicing and 3D modeling. The detailed structural parameters of the connector, including the dimensions of the metal and dielectric regions, are measured by disassembling and slicing the connector to build a 3D standalone connector SI simulation model (without fixtures). The Djordjevic-Sarkar model for frequency-dependent dielectric material and the Hammerstad-Jensen model for copper foil roughness are used to achieve good simulation accuracy across the entire frequency range. [4] [5]

The dielectric material parameters are defined using the Djordjevic-Sarkar model for AI-driven 3D FEM optimization simulations. The optimization goal is based on the passive parameters of the S-parameters of the tested connector. Through optimization, the ε_∞, $\Delta\varepsilon$, m_1, and m_2 parameter values in the Djordjevic-Sarkar model are determined, finally characterizing the frequency dependence of the complex dielectric constant ε.

$$\varepsilon = \varepsilon_\infty + \Delta\varepsilon \cdot \frac{1}{m_2 - m_1} \cdot log_{10}\left(\frac{10^{m_2} + if}{10^{m_1} + if}\right) \tag{3}$$

$$\varepsilon = \varepsilon_r \cdot (1 - i \cdot tan\delta) \tag{4}$$

Here, ε_∞ is the relative permittivity at high frequencies, $\Delta\varepsilon$ is the difference between the dielectric constants at low and high

frequencies, m_1 and m_2 are parameters that control the logarithmic frequency range. The frequency-dependent relative permittivity ε_r and tanδ characteristics of the Djordjevic-Sarkar model are shown in Figure 5.

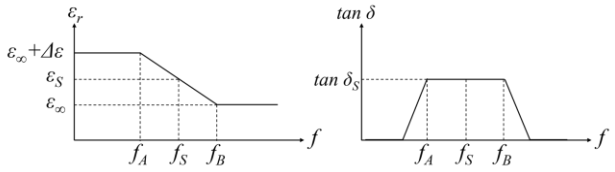

Figure 5. The frequency-dependent ε_r and tan δ characteristics of the Djordjevic-Sarkar model.

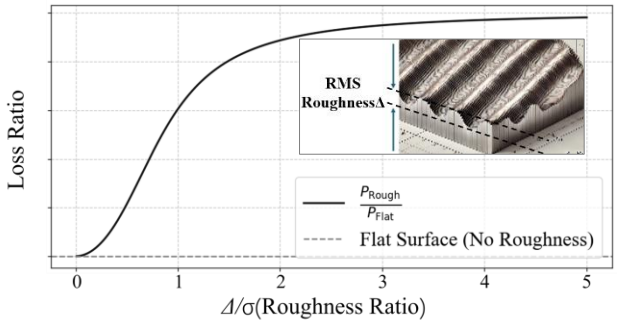

Figure 6. Impact of surface roughness on power loss.

$$Loss\ Ratio = \frac{P_{Rough}}{P_{Flat}} = 1 + \frac{2}{\pi} arctan\left[1.4\left(\frac{\Delta}{\sigma}\right)^2\right](SF - 1) \quad (5)$$

To model the conductor loss of the connector pins under the high-frequency skin effect, the connector modeling process incorporates roughness parameters. A surface profilometer is used to measure the 3D morphology of the metal surface of the pins and calculate the RMS roughness Δ. The skin depth σ is obtained through 3D electromagnetic field simulations of the connector, and the Scaling Factor (SF) is derived from data provided by the vendor. P_{Rough} and P_{Flat} represent the signal power on rough and smooth surfaces, respectively, and their ratio is used to quantify the metal roughness loss factor, as shown in Figure 6 and Equation (5).

Step3: Validate the material parameter fitting results. Comparison with the tested S-parameters shows good agreement between the simulated and measured amplitudes of SDD21, SDD11, and the phase of SDD21 across the full frequency range of 0~20 GHz, as shown in Figure 7, completing the accuracy calibration of the initial model.

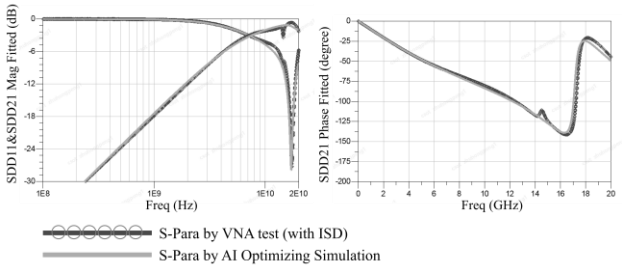

Figure 7. SDD11 & SDD21 fitting calibration results.

3.2. CNT Model Bandwidth Validation

The connector operates over a wide frequency range. For power and low-speed signal interfaces, this study performed a feasibility validation using a low-frequency lumped RLGC model. For high-speed signal interfaces, due to the transmission line effects, the lumped parameter simulation does not provide sufficient accuracy, so an S-parameter model is used to describe the distribution parameters across the entire frequency range.

(a) RLGC Model Feasibility Analysis

When the connector size is much smaller than the signal wavelength, a lumped parameter model can be used for analysis. The connector's lumped parameters at multiple frequency points are extracted using 3D simulation software and fitted through interpolation. Comparison of the input impedance and insertion loss results shows that the bandwidth of a single-section RLGC model is approximately 1.5 GHz, while increasing to 40 sections extends the bandwidth to around 3 GHz, as shown in Figure 8 (a)(b). The fitting error primarily arises from the non-uniformity of the connector's cross-sectional structure, and for irregular structures, 3D FEM analysis is used to obtain high-bandwidth, high-precision results.

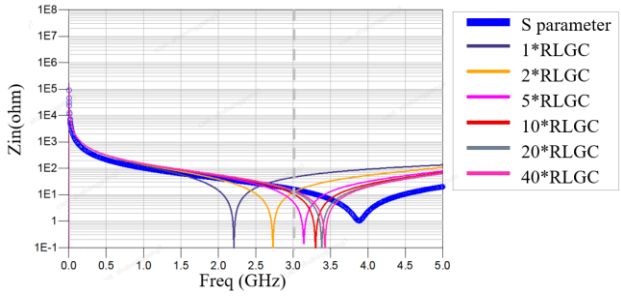

Figure 8. (a) Input impedance Zin of the RLGC model with different number of cascaded sections.

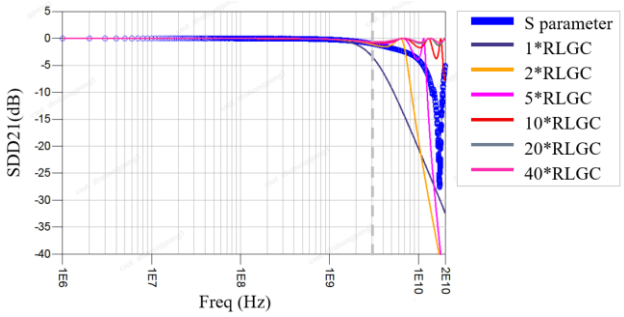

Figure 8. (b) Insertion loss SDD21 of the RLGC model with different number of cascaded sections.

(b) High-Frequency Effect Analysis

The high-frequency characteristics of the connector's stub need to account for transmission line effects. When a high-speed incident signal reaches the open end of the stub, complete reflection occurs, and the reflected signal combines with the incident signal, resulting in energy interaction. When the round-trip delay of the stub is an odd multiple of the signal's half-period, the phase difference between the original and reflected signals is 180 degrees, leading to maximum phase cancellation, corresponding to the periodic resonance on the SDD21 insertion loss curve:

$$f_{res} = (2n+1)\frac{c}{4*\sqrt{\varepsilon_{eff}}*L_{Stub}} \quad (6)$$

Here, L_Stub is the total length of the stub, c is the speed of light in vacuum, ε_{eff} is the effective relative permittivity of the material, and n represents the sequence of resonance point.

Considering the signal bandwidth is 5 times the base frequency, in order to ensure that resonance does not affect high-speed signals, the resonant frequency should be at least twice the signal bandwidth. Based on this, the design requirements for the connector pin stub length can be derived as follows:

$$L_{Stub} < \frac{c}{20*\sqrt{\varepsilon_{eff}}*DR} \quad (7)$$

The results show that as the signal data rates(DR) increases, the wavelength shortens, and the requirement for stub length becomes more stringent. The connector's stub is a key factor limiting its transmission bandwidth. In this study, the connector's stub length is approximately 100 mils. The simulation results show that the first and second resonant frequencies of SDD21 are 17.3 GHz and 38.8 GHz, respectively (Figure 8). Considering the lower actual value of ε, the theoretical bandwidth limit is calculated to be approximately 3 Gbps. It is evident that the connector's stub is rapidly becoming a major bottleneck for the high-speed channel bandwidth in display panel products!

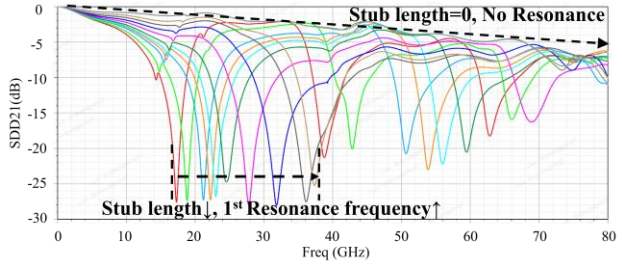

Figure 8. The relationship between the SDD21 resonantce and stub length. L_{Stub} =[100mil, 0 mil], step=-10mil

The study also found that the connector's stub width affects the resonant points. The stub width does not affect the distribution of resonant frequencies, but it has a positive effect on resonance strength. Wider stub trace lead to a greater impedance drop, by reducing the connector pin width, impedance can be improved and insertion loss can be reduced. [6]

In summary, through simulation analysis, reducing the stub length and width can significantly improve the connector's performance and effectively increase its transmission bandwidth to several tens of Gbps. The high-frequency passive characteristics of the connector's stub are described using an S-parameter model, which offers excellent wideband advantages.

4. XGBoost Training and Prediction

This study employs an efficient prediction model based on XGBoost regression and Bayesian optimization, with the goal of predicting key performance indicators of connector signal integrity, including insertion loss, return loss, TDR impedance, eye height, eye width, and jitter RMS values at different frequencies, as shown in Figure 9. Bayesian optimization is used to automatically adjust hyperparameters of the XGBoost model, such as learning rate, tree depth, number of trees, and subsample ratio, with iterative calculations to improve the model's prediction accuracy. [7]

Specifically, noise addition and parameter perturbation were applied to the simulation results. Gaussian noise with a standard deviation was added to the input features and output labels to simulate signal interference and measurement errors. Additionally, a ±5% perturbation was applied to features such as dielectric constant, loss tangent, and frequency to simulate the effects of environmental changes and process variations. [8]

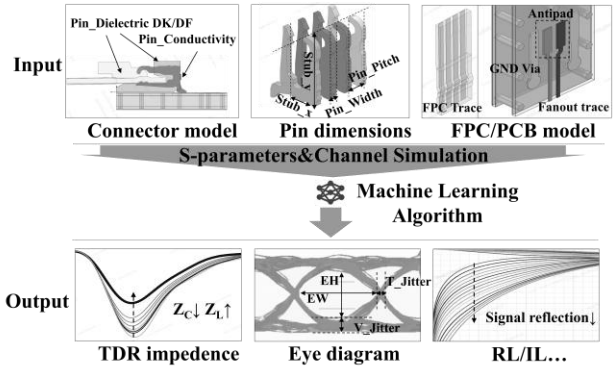

Figure 9. XGBoost model input and output architecture.

The model performance was evaluated using multiple metrics, including Mean Squared Error (MSE), Root Mean Squared Error (RMSE), and R-squared (R^2). The Figure 10 (a) (b) show that the insertion loss and return loss predicted by the XGBoost model match the actual test results well, with an R^2 of 0.99 on the test set, indicating high prediction accuracy. Furthermore, the XGBoost model's regression coefficient improved by 13.8% compared to the DNN (Deep Neural Network) model on the test set as shown in Figure 11.

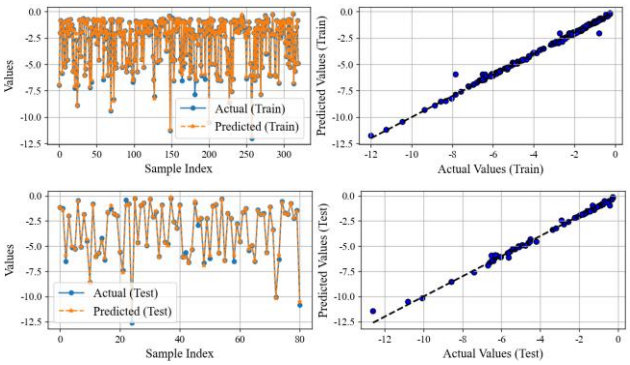

Figure 10. (a) IL training and prediction results.

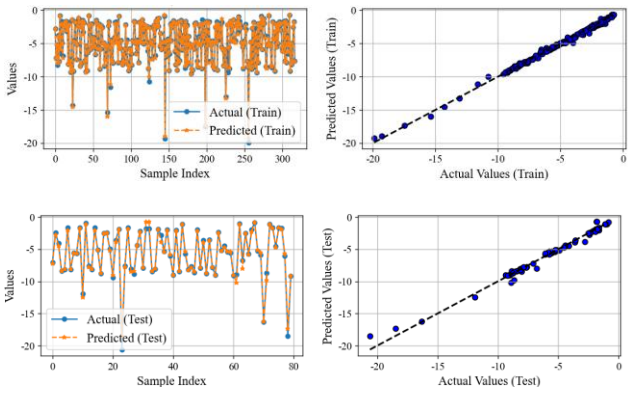

Figure 10. (b) RL training and prediction results.

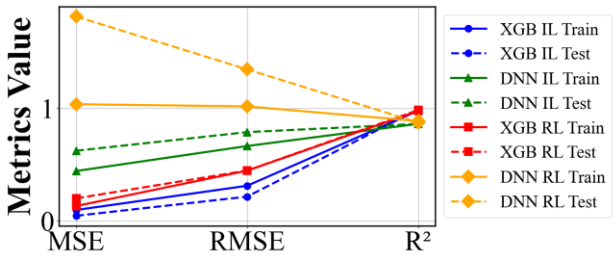

Figure 11. Model performance comparison (IL and RL)

To account for the effects of temperature and humidity, this study uses 3DFEM simulations to obtain a dataset for model training, specifically simulating the variation characteristics of dielectric constant, loss tangent, and conductivity under different temperature and humidity conditions. For assembly errors, the model is trained and validated using a feature set that includes insertion angle and pin contact depth, in order to assess the impact of assembly deviations on the connector's performance.

5. Conclusion and Applications

This study proposes a method combining XGBoost regression and Bayesian optimization for efficiently evaluating connector signal integrity. The method retains training efficiency while using Bayesian optimization to find the optimal combination of hyperparameters. The R^2 on the test set reaches 0.99, an improvement of 13.8% over traditional DNN methods, demonstrating high prediction accuracy and generalization ability.

This machine learning-based prediction method significantly reduces reliance on traditional simulation and physical testing in connector design, greatly improving design efficiency and performance evaluation accuracy. Eye height quality improves by 66.79% at 25Gbps, as shown in Figure12 (c), and the passive simulation speed is approximately 66 times faster than traditional 3D FEM simulations, as shown in Figure13. This method provides an effective solution for future high-bandwidth connector SI simulation and optimization design, supporting the advancement of high-speed interconnect technologies for display products.

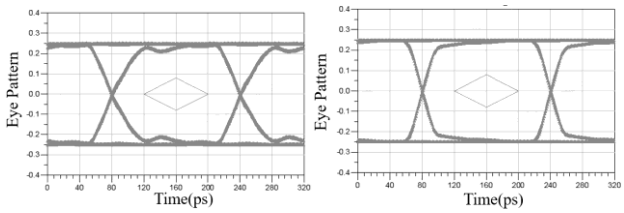

Figure 12 (a). Eye diagram before and after optimization at 6.25Gbps.

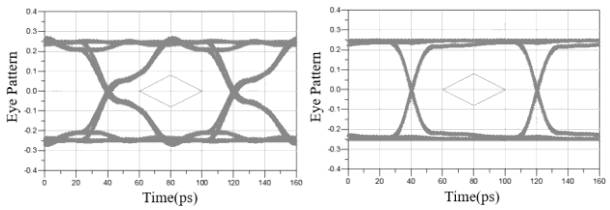

Figure 12 (b). Eye diagram before and after optimization at 12.5Gbps.

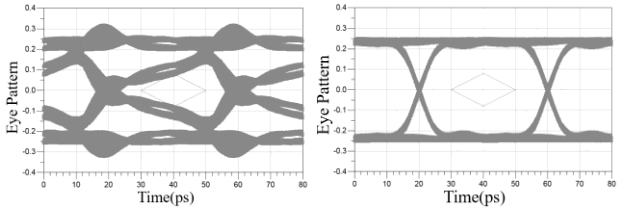

Figure 12 (c). Eye diagram before and after optimization at 25Gbps.

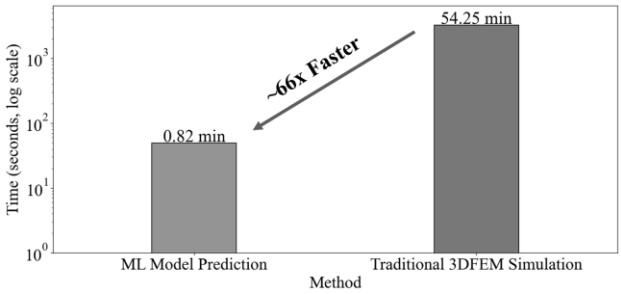

Figure 13. ~66x improvement in connector simulation efficiency

6. References

1. Miller, M., & Thompson, R. (2022). "Advances in High-Speed Digital Design and Signal Integrity." IEEE Transactions on Components, Packaging and Manufacturing Technology, 12(6), 1045-1055.
2. Anderson, D., & Parker, L. (2021). "Effects of Surface Roughness and Dielectric Materials on High-Speed Interconnect Performance." Proceedings of DesignCon 2021, 120-125.
3. Zhang, Y., & Li, X. (2020). "Connector slicing and de-embedding for SI simulation model calibration." DesignCon Proceedings, 2020, 123-134.
4. Djordjevic, A., & Sarkar, T. K. (1999). "A new model for characterizing the dispersion and losses in transmission lines." IEEE Transactions on Microwave Theory and Techniques, 47(12), 2426-2434.
5. Jensen, J. B., & Hammerstad, E. (1985). "Transmission Line Models for Microstrip and Other Interconnects." Proceedings of the IEEE International Microwave Symposium (IMS), 1985, 202-205.
6. Kim, Y., & Lee, J. (2018). "Impact of Connector Stub Resonance on Signal Loss and Bandwidth in High-Speed Networks." IEEE Journal of Electromagnetic Waves and Applications, 32(8), 1062-1070.
7. Miller, D., & Thompson, R. (2021). "Optimizing Signal Integrity Prediction Using XGBoost and Neural Networks: A Comprehensive Evaluation." IEEE Transactions on Components, Packaging, and Manufacturing Technology, 11(8), 1350-1360.
8. Brown, S., & Kumar, P. (2019). "Impact of environmental variations on signal integrity: A simulation-based study." DesignCon Proceedings 2019, 123-133.